

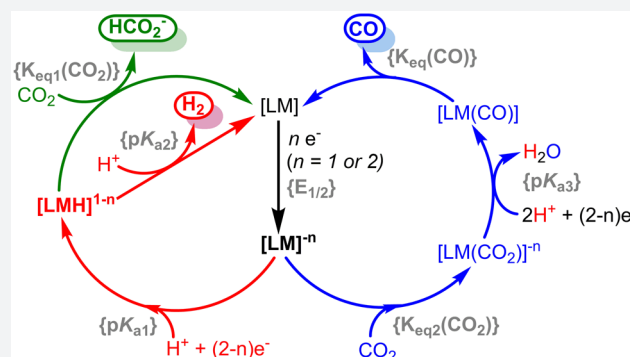
# Thermodynamic Considerations for Optimizing Selective CO<sub>2</sub> Reduction by Molecular Catalysts

Jeffrey M. Barlow and Jenny Y. Yang\*<sup>✉</sup>

Department of Chemistry, University of California, Irvine, California 92697, United States

**S** Supporting Information

**ABSTRACT:** Energetically efficient electrocatalysts with high product selectivity are desirable targets for sustainable chemical fuel generation using renewable electricity. Recycling CO<sub>2</sub> by reduction to more energy dense products would support a carbon-neutral cycle that mitigates the intermittency of renewable energy sources. Conversion of CO<sub>2</sub> to more saturated products typically requires proton equivalents. Complications with product selectivity stem from competitive reactions between H<sup>+</sup> or CO<sub>2</sub> at shared intermediates. We describe generalized catalytic cycles for H<sub>2</sub>, CO, and HCO<sub>2</sub><sup>−</sup> formation that are commonly proposed in inorganic molecular catalysts. Thermodynamic considerations and trends for the reactions of H<sup>+</sup> or CO<sub>2</sub> at key intermediates are outlined. A quantitative understanding of intermediate catalytic steps is key to designing systems that display high selectivity while promoting energetically efficient catalysis by minimizing the overall energy landscape. For CO<sub>2</sub> reduction to CO, we describe how an enzymatic active site motif facilitates efficient and selective catalysis and highlight relevant examples from synthetic systems.



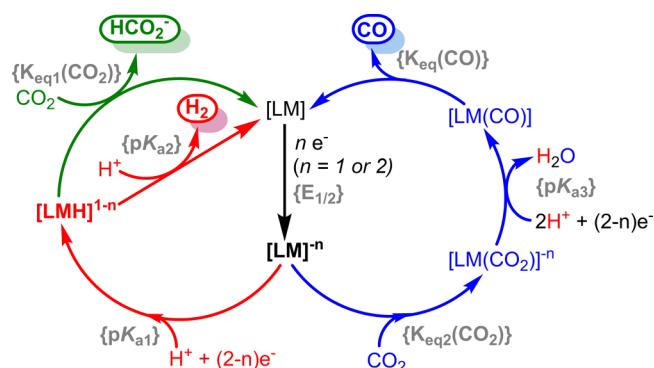
The electrocatalytic reduction of CO<sub>2</sub> is a direct route to sustainable fuel production from renewable electricity.<sup>1–3</sup> Although protons are required to convert CO<sub>2</sub> to chemical fuels, direct proton reduction to H<sub>2</sub> siphons electrons away from CO<sub>2</sub> reduction, decreasing the Faradaic yield of carbon-containing products.<sup>4,5</sup>

Nonselective reduction is commonly the result of the competitive reactions with either H<sup>+</sup> or CO<sub>2</sub> at key intermediates that ultimately lead to divergent pathways and products (Scheme 1). Some of the earliest work investigating the mechanism of molecular electrocatalysts for CO<sub>2</sub> reduction suggested differential reactivity at common intermediates.<sup>6</sup> Additional studies quantified the relative reactivity of H<sup>+</sup> and

CO<sub>2</sub> at these proposed electrocatalytic intermediates.<sup>7–16</sup> With the resurgence of interest in CO<sub>2</sub> reduction over the past decade, new mechanistic studies and catalysts have generated fresh insights into the varying factors that contribute to product selectivity.<sup>3,17–29</sup>

Nonselective reduction is commonly the result of the competitive reactions with either H<sup>+</sup> or CO<sub>2</sub> at key intermediates that ultimately leads to divergent pathways and products.

Scheme 1



Our analysis is focused on the thermodynamic considerations for key steps in the most commonly proposed catalytic cycles for the hydrogen evolution reaction (HER) and carbon dioxide reduction reaction (CO<sub>2</sub>RR) to formate (HCO<sub>2</sub><sup>−</sup>) and carbon monoxide (CO) by inorganic molecular electrocatalysts. Our evaluation includes general trends in catalyst properties and their broad impact on reactivity. We examine free energy considerations for the reaction of H<sup>+</sup> and CO<sub>2</sub> with proposed catalyst intermediates and the potential barriers for product release. These considerations provide guidelines for

Received: January 30, 2019

Published: March 12, 2019

achieving selectivity at divergent reaction paths and are also essential for improving catalytic activity. Although our discussion is not focused on kinetic considerations, we note that intermediate steps in catalysis with high or low free energies intrinsically contribute to kinetic barriers in addition to the overall energetic efficiency (expressed in the overpotential). Thus, a quantitative understanding of the free energy contributions of each step is necessary to flatten the energy landscape and optimize activity.

We note that our analysis utilizes reported catalysts as examples but is not intended to be a complete description of the field. Instead, we refer the reader to more comprehensive reviews of molecular electrocatalysts for CO<sub>2</sub> reduction that have recently been published.<sup>30–32</sup>

**Overall Reaction Scheme.** A generalized scheme for the catalytic reduction of H<sup>+</sup> and CO<sub>2</sub> to H<sub>2</sub>, HCO<sub>2</sub><sup>−</sup>, and CO is shown in Scheme 1. Although other catalytic routes are possible, Scheme 1 represents the most frequently cited mechanisms. Upon electron transfer at a certain redox potential {E<sub>1/2</sub>}, the reduced intermediate can either protonate to form a metal hydride or directly activate CO<sub>2</sub>. In the *protonation-first pathway* (red), a metal hydride is formed which can react either with a second proton to form H<sub>2</sub>, or with CO<sub>2</sub> to produce formate (green). Conversely, CO is typically the product in a *CO<sub>2</sub>-activation-first pathway* (blue). Each of these possibilities will be described separately.

**Metal Hydride Formation.** The *protonation-first pathway* requires the ability to form a stable metal hydride upon protonation. The free energy of protonation is the difference in pK<sub>a</sub> between the proton acceptor ({pK<sub>a1</sub>}), or that of the targeted

$$\Delta G = -2.303RT(pK_{a(\text{ext})} - pK_{a1}) \quad (1)$$

metal hydride intermediate) and proton donor ({pK<sub>a(ext)</sub>}, or external acid source) as expressed in eq 1. We intuitively expect more electron-rich metal centers to have more negative reduction potentials and be more Brønsted basic (higher metal hydride pK<sub>a</sub> values).

The measured pK<sub>a</sub> values of metal hydrides with reported reduction potentials {E<sub>1/2</sub>} in acetonitrile are plotted in Figure 1.<sup>33–53</sup> The series represents a broad span of metal hydrides in different ligand environments (see Tables S1–S3 in the Supporting Information). Following the expected trend, more reducing metal centers are also stronger Brønsted bases. Since pK<sub>a</sub> is a metric of heterolytic M–H bond free energy, Figure 1

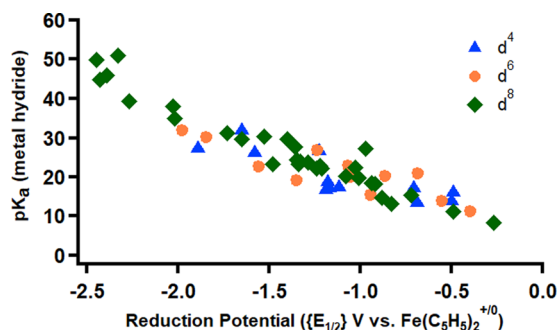


**Figure 1.** pK<sub>a</sub> values of metal hydrides plotted versus the reduction potential required to access their conjugate bases. Blue triangles, orange circles, and green diamonds represent d<sup>4</sup>, d<sup>6</sup>, and d<sup>8</sup> metal hydrides, respectively. Compiled from refs 33–53.

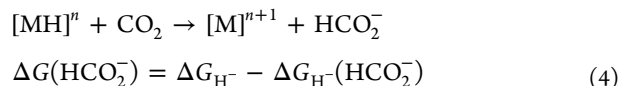
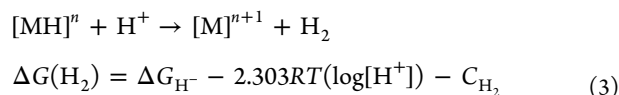
also depicts the linear free energy relationship between redox potential and the bond dissociation free energy of the M–H bond.

R. H. Morris recently reported a valuable empirical model for calculating metal hydride pK<sub>a</sub> values based on ligand acidity constants.<sup>54,55</sup> A review also compiled experimentally measured and calculated pK<sub>a</sub> values for a broad range of metal hydrides (as well as dihydrogen complexes).<sup>56</sup> Additionally, he notes that since M–H bond dissociation free energies are typically ~60 kcal/mol,<sup>33–37,57,58</sup> the pK<sub>a</sub> values of metal hydrides are expected to correlate with the redox potential of the conjugate base as seen in Figure 1.<sup>54</sup>

**H<sub>2</sub>/HCO<sub>2</sub><sup>−</sup> Formation.** Upon metal hydride formation, it can react with either another proton or CO<sub>2</sub>. M. R. Dubois and D. L. Dubois first described how the free energy for the reactions of a metal hydride with H<sup>+</sup> or CO<sub>2</sub> at a metal hydride is determined by the hydricity (ΔG<sub>H<sup>−</sup></sub>, eq 2) of the metal hydride.<sup>59,60</sup> The hydricity is dependent on the two-electron reduction potential and pK<sub>a</sub> of the transition metal hydride along with the reduction potential for H<sup>+</sup>/H<sup>−</sup> in the respective solvent.<sup>48,61,62</sup> As a result, hydricity values correlate with the average two-electron reduction potential of the metal (Figure S1).

The free energy for protonation of a metal hydride to evolve H<sub>2</sub> (ΔG(H<sub>2</sub>)) is shown in eq 3; it is dependent on its hydricity (ΔG<sub>H<sup>−</sup></sub>), the pK<sub>a</sub> of the external proton donor, and the heterolytic cleavage energy of H<sub>2</sub> (C<sub>H<sub>2</sub></sub>, a solvent-dependent constant). The free energy to reduce CO<sub>2</sub> to formate (eq 4) is dependent on the hydricity of the metal hydride “donor” (ΔG<sub>H<sup>−</sup></sub>) and the hydricity of formate (ΔG<sub>H<sup>−</sup></sub>(HCO<sub>2</sub><sup>−</sup>)), the “acceptor”. The free energy of hydride transfer (ΔG(HCO<sub>2</sub><sup>−</sup>)) relates directly to {K<sub>eq1</sub>(CO<sub>2</sub>)} in Scheme 1. Several recent perspectives have discussed these relationships in depth.<sup>61–63</sup>

The pK<sub>a2</sub> in Scheme 1 delineates the proton activity in which ΔG(H<sub>2</sub>) is close to zero, or ergoneutral. Using external acids with a lower pK<sub>a</sub> than pK<sub>a2</sub> will result in H<sub>2</sub> evolution



whereas the metal hydride will be stable to protonation with acids of a higher pK<sub>a</sub>.<sup>64–66</sup> Since minimization of free energy leads to efficient catalysis, eq 3 was applied to optimize a class of catalysts for H<sub>2</sub> evolution.<sup>67</sup> A characteristic of a catalyst with a flattened energetic landscape is reversible reactivity (i.e., hydrogen evolution and oxidation), which was also illustrated in this class.<sup>68–70</sup>

An interesting aspect of eqs 3 and 4 is that the free energy of protonation of a metal hydride is dependent on the pK<sub>a</sub> of the proton donor, while the reaction with CO<sub>2</sub> is not. As a result, there are conditions in which the reaction of a metal hydride with CO<sub>2</sub> is exergonic while protonation to form H<sub>2</sub> is endergonic. In these cases, if the pK<sub>a</sub> of the proton donor is sufficiently low enough to form the metal hydride, selective CO<sub>2</sub> reduction can be accessed via thermodynamic consid-

erations alone. These conditions exist because CO<sub>2</sub> reduction to formate is a 1H<sup>+</sup>, 2e<sup>-</sup> process above the pK<sub>a</sub> of formic acid, while H<sup>+</sup> reduction to H<sub>2</sub> is a 2H<sup>+</sup>, 2e<sup>-</sup> process across all pK<sub>a</sub> values. As a result, the thermodynamic potential for each reaction has a differential dependence on proton activity. We recently published a more detailed description on this topic.<sup>64</sup>

if the pK<sub>a</sub> of the proton donor is sufficiently low enough to form the metal hydride, selective CO<sub>2</sub> reduction can be accessed via thermodynamic considerations alone

We also note the thermodynamic values in eqs 2 and 4 are solvent-dependent, but do not quantitatively change to the same magnitude in different solvents.<sup>41,61,71–76</sup> For example, while the hydricity for metal hydrides and formate decreases from organic solvents to water (or become better donors), formate's hydricity decreases to a lesser extent. As a result, some metal hydrides that are insufficiently hydric to reduce CO<sub>2</sub> in organic solvents will do so in water.<sup>71,72,77</sup>

In accordance to the Sabatier principle, the interactions between the catalyst and substrate/product are also important. A significant interaction between the catalyst resting state and formate would make a favorable (negative) contribution to the free energy in eq 4, permitting CO<sub>2</sub> reduction with weaker hydride donors. However, the interaction will also inhibit product release and catalyst turnover. Most putative hydride intermediates in successful CO<sub>2</sub> reduction catalysts are composed of electron-rich mid or late transition metals<sup>18,26,64,78–81</sup> which only weakly bind formate, so product release is not rate-limiting.

**CO Production.** The CO<sub>2</sub>-activation-first pathway (blue in Scheme 1) requires CO<sub>2</sub> activation to outcompete protonation at the reduced metal center. While very little quantitative data exists on CO<sub>2</sub> binding constants {K<sub>eq2</sub>(CO<sub>2</sub>)} at reduced metal centers, a small but instructive data set exists for Co(I) tetraaminemacrocycles.<sup>82</sup> In the absence of ligand steric effects, log{K<sub>eq2</sub>(CO<sub>2</sub>)} correlates with the Co(II/I) redox potential (Figure 2).<sup>82–84</sup> The relationship is also intuitive, where more electron-rich (reducing) metal centers activate CO<sub>2</sub> more strongly. In fact, no single transition metal site is known to react with CO<sub>2</sub> at potentials positive of -1.2 V vs Fe(C<sub>5</sub>H<sub>5</sub>)<sub>2</sub><sup>+0</sup> in organic solvents.<sup>30–32</sup>

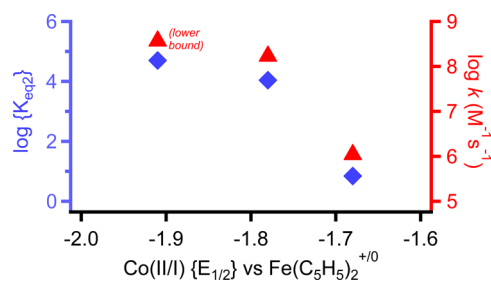


**Figure 2.** Relationship between {E<sub>1/2</sub>} of Co(I) macrocyclic complexes and thermodynamic (log{K<sub>eq2</sub>}) and kinetic (log k) reactivity with CO<sub>2</sub>. Data from ref 82.

The negative potentials required to activate CO<sub>2</sub> have several undesirable side effects for overall catalyst selectivity, efficiency, and rate. As illustrated in Figure 1, more reducing metal sites are also more Brønsted basic (with the caveat that protonation to form a metal hydride requires two-electron oxidation of the complex, which is not always accessible). Thus, more reducing metal centers favor both the CO<sub>2</sub>-activation-first and the protonation-first pathways.

Another complicating factor is that in organic solvents the product, CO, is often a better ligand than CO<sub>2</sub>. Thus, increasing the electron density of the metal for CO<sub>2</sub> activation often results in a more stable M–CO complex later in the catalytic cycle, inhibiting turnover. CO release has been shown to be rate-limiting in several known catalysts.<sup>84–88</sup> (We note that this is not always the case; an earlier study found CO<sub>2</sub> and CO equilibrium binding constants to cobalt macrocycles were competitive in water.)<sup>14</sup>

As a result, catalyst design for optimal CO<sub>2</sub> reduction to CO requires an intimate understanding of how CO<sub>2</sub>, CO, and H<sup>+</sup> interact with reduced metal centers. The importance of these parameters was delineated by Schneider, Fujita, and co-workers in 2012 based on their experimental work with cobalt macrocycles.<sup>82,84,87</sup> Their analysis inspired our study on a series of isostructural cobalt pincer complexes, the results of which are summarized in Table 1.<sup>89</sup> Cobalt complexes with

**Table 1.** Interaction of CO<sub>2</sub>, CO, and H<sup>+</sup> for an Isostructural Series of Cobalt Pincer Complexes (Data from Ref 89)

L	P <sup>C</sup> N <sup>C</sup> P	P <sup>N</sup> N <sup>N</sup> P	P <sup>O</sup> N <sup>O</sup> P
E <sub>1/2</sub> , LCo(II/I) <sup>a</sup>	-1.03 V	-0.88 V	-0.61 V
k[CO <sub>2</sub> ] (s <sup>-1</sup> ), [LCo] <sup>b</sup>	10 <sup>2-3</sup>	10 <sup>2-3</sup>	no reaction
[LCo(CO)] <sup>+</sup> , ν (cm <sup>-1</sup> )	1911	1923	1936
pK <sub>w</sub> <sup>c</sup> [LCo]	28		32

<sup>a</sup>vs Fe(C<sub>5</sub>H<sub>5</sub>)<sub>2</sub><sup>+0</sup> in CH<sub>3</sub>CN. <sup>b</sup>Reactivity with CO<sub>2</sub> occurs upon reduction of the Co(I) complex, which is electrochemically irreversible. E<sub>1/2</sub> for the reversible Co(II/I) couple is provided to illustrate the electronic trend. <sup>c</sup>Calculated for corresponding protonated complex.

more electron-donating ligands result in more negative reduction potentials and greater reactivity toward CO<sub>2</sub> (see Table 1). We were unable to obtain accurate rate constants, but the overall trend is similar to that observed in the cobalt macrocycles (Figure 2). The Co–(CO) bond strength, measured by the vibrational stretch (ν) of the CO bond by infrared spectroscopy, also increased with decreasing reduction potential.

The free energy relationships for metals and their association with CO<sub>2</sub>, CO, and H<sup>+</sup> are comparable to scaling relationships more commonly used for analyzing heterogeneous catalysts. In this case, we find the general trends that relate redox potential with reactivity for the three key substrates follow opposing



directions for catalyst optimization. Similar trends were also described for heterogeneous electrocatalysts.<sup>90</sup>

A generalized energy landscape for a single-site activation of CO<sub>2</sub> to CO is depicted in black in Figure 3. A strongly

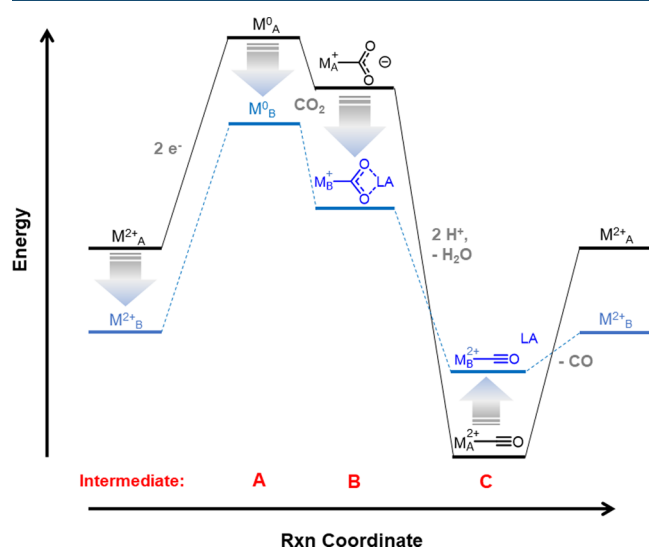


**Figure 3.** Free energy landscape for a single-site catalyst for CO<sub>2</sub> reduction to CO (black) and a catalyst that utilizes a cooperative interaction (blue) to stabilize the metal carboxylate intermediate B.

reducing (and thus higher energy) metal site (intermediate A) is utilized to activate the electrophilic carbon in CO<sub>2</sub>. CO<sub>2</sub> can bind to metals in a few different orientations. The  $\eta^1$  coordination is unstable in synthetic transition metal complexes<sup>91,92</sup> (although if there is another vacant coordination site, it can bind  $\eta^2$ ).<sup>93–96</sup> The highly nucleophilic oxygen atoms on unstable metal carboxylates (intermediate B) can promote ligand decomposition<sup>97</sup> or disproportionation with another equivalent of CO<sub>2</sub> to give CO and CO<sub>3</sub><sup>2-</sup>.<sup>20,98–103</sup> A characteristic of an unstable metal carboxylate is extreme Brønsted basicity (high {pK<sub>a3</sub>}), which has been observed in some catalytic systems that scavenge protons from adventitious water or electrolyte.<sup>104–107</sup> If protonation and reduction of the metal carboxylate (intermediate B) is successful in cleaving a C–O bond, more electron-rich metals will result in a greater energetic barrier for CO release (intermediate C).

Given these factors, it is clear that activation of CO<sub>2</sub> at more positive potentials confers several benefits. In addition to catalysis at a milder potential, it inhibits the *protonation-first pathway* by lowering the Brønsted basicity of the metal while favoring product release.

Perhaps it is not surprising that a strategy for activating CO<sub>2</sub> at mild potentials can be found in nature, where efficient redox catalysis for energy transduction is a matter of survival. The electrocatalytic activity of Ni-CODH I, a carbon monoxide dehydrogenase of the anaerobic *Carboxydotherrmus hydrogeniformans* (*Ch*), displays reversible electrocatalysis of CO<sub>2</sub> to CO at high rates at the thermodynamic potential (no overpotential), or  $-520$  mV vs SHE at pH 7.<sup>108</sup> The X-ray crystallographic structure of the enzyme under reducing conditions in the presence of CO<sub>2</sub> suggests cooperative binding by Ni and Fe, shown in Figure 4.<sup>109</sup> Electrophilic activation of CO<sub>2</sub> occurs at the redox active and Lewis basic reduced Ni<sup>0</sup>, while the adjacent Fe<sup>2+</sup> participates in nonredox substrate activation. Thus, the active site capitalizes on a

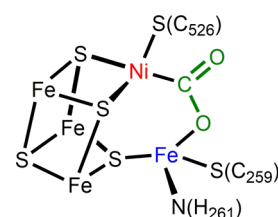


**Figure 4.** Active site of reduced *Ch* Ni-CODH II in the presence of CO<sub>2</sub> characterized by X-ray crystallography (adapted from ref 109).

secondary interaction to cooperatively bind CO<sub>2</sub> instead of a single metal site, contributing to its high rate and low overpotential.<sup>32,109–111</sup>

An energetic analysis of a cooperative CO<sub>2</sub> activation mechanism is shown in blue in Figure 3. Cooperative activation stabilizes the carboxylate intermediate, making a favorable free energy contribution to CO<sub>2</sub> activation. This results in reactivity at more positive potentials, which also destabilizes the subsequent metal carbonyl product, facilitating product release. Not represented in Figure 3 is the *protonation-first pathway*, but we would expect it to be less favorable as the Brønsted basicity of the reduced metal decreases, contributing to enhanced selectivity.

There is evidence that several synthetic catalysts cooperatively activate CO<sub>2</sub>, which benefits their rate and/or selectivity. Bimetallic activation of CO<sub>2</sub> is proposed in a synthetic dipalladium system.<sup>30</sup> Single-site palladium complexes with a triphosphine ligand display a linear free energy relationship (LFER) between  $K_{eq}(\text{CO}_2)$  and redox potential.<sup>67</sup> Addition of a hydrogen-bonding interaction or a second metal disrupted the LFER, leading to faster catalytic CO<sub>2</sub> reduction at a milder potential. Optimization of the cooperative interaction increased the rate of CO<sub>2</sub> to CO catalysis by 3 orders of magnitude compared to the monomer while lowering the overpotential almost 200 mV.<sup>59,112–115</sup> Additionally, the Faradaic efficiency improved from 10:90 CO:H<sub>2</sub> to 85:15 CO:H<sub>2</sub> upon introduction of the second metal center.<sup>113,115</sup>

However, the two symmetric homobimetallic sites have similar reduction potentials, which results in unproductive metal–metal bond formation, deactivating the catalyst. By using two different metals, the [NiFe] center of *Ch* Ni-CODH, promotes selective redox chemistry at the Ni site. Several other synthetic transition metal CO<sub>2</sub> reduction catalysts have shown substantial evidence for bimetallic CO<sub>2</sub> activation.<sup>86,97,116–124</sup> A dicobalt carboxylate complex was also structurally characterized from a cobalt macrocyclic catalyst.<sup>125</sup> We note several heterobimetallic systems utilize strong oxophilic Lewis acids to activate CO<sub>2</sub>,<sup>116,126</sup> in some cases, the latter can bind the oxygen too tightly for catalyst turnover.

Other successful catalysts attribute improved activity to other types of cooperative CO<sub>2</sub> activation. Early mechanistic and computational studies for the catalysts [Ni(cyclam)]<sup>+</sup> and cobalt macrocycles indicate the importance of the protons on the macrocycle amines for facilitating CO<sub>2</sub> binding.<sup>9,127</sup> Savéant and co-workers have also shown that the incorporation of phenol moieties in the secondary coordination sphere of a previously investigated iron porphyrin complex results in a 50-fold rate increase at an overpotential 360 mV lower than the corresponding anisole substituted system.<sup>128</sup> Most recently, Dey and co-workers reported a low overpotential electrocatalyst which incorporates a proposed S–H functionality appropriately positioned to stabilize a metal carboxylate.<sup>22</sup> A

key feature of these hydrogen-bonding interactions is that they are positioned appropriately to facilitate CO<sub>2</sub> binding (interaction with an O atom on the carboxylate) without enhancing direct proton delivery to the metal, which would favor the *protonation-first pathway*. Another system with proximal secondary amines was found to enhance protonation by generating a local hydrogen-bonding environment, even if they do not assist in CO<sub>2</sub> binding.<sup>129</sup> Although we are not discussing the second protonation event required to liberate water in detail, another possible route to H<sub>2</sub> is direct protonation of the metal carboxylic acid. Careful positioning of secondary sphere hydrogen-bonding functionalities is important for circumventing this possibility.

It has been suggested that cationic functionalities also lower the energetic requirement to access a metal carboxylate intermediate. Savéant and coworkers utilized cationic ammonium substituents to promote CO<sub>2</sub> reduction through electrostatic stabilization of a bound carboxylate species.<sup>130</sup> Iron porphyrin complexes featuring *o*-NMe<sub>3</sub><sup>+</sup> substituents function at 230 mV lower potential than the corresponding *p*-NMe<sub>3</sub><sup>+</sup> substituted complex, while operating at 100 times the rate. In contrast, catalyst activity was suppressed when the cationic amines were replaced with anionic sulfonate moieties, highlighting the effects of electrostatic interactions on CO<sub>2</sub> catalysis.<sup>130</sup> Electrostatic interactions have more recently been utilized for a similar beneficial effect in rhenium bipyridine systems.<sup>131</sup>

In addition to increasing the reaction rate and decreasing the required overpotential for catalysis, CO<sub>2</sub> activation involving cooperative interactions can also affect product selectivity. Large enhancements in CO selectivity have been observed in systems featuring hydrogen-bonding,<sup>129,132,133</sup> bimetallic,<sup>113</sup> and electrostatic interactions.<sup>134</sup>

Although synthetic catalysts have successfully utilized cooperative CO<sub>2</sub> activation to enhance their activity or selectivity, they have yet to achieve the lofty catalytic metrics exhibited by Ni-CODH I. We expect there are more secrets to be discovered for how the active sites of the carbon monoxide dehydrogenases (including the less studied MoCu class) balance key kinetic and thermodynamic factors for efficient, fast, and selective catalysis.

## CONCLUSION

Efficiency, rate, and product selectivity are key figures of merit for electrocatalysts. Intermediate steps with large changes in free energy pay an energetic and intrinsic kinetic cost. A quantitative understanding of the free energy of each step in the catalytic cycle can be applied to minimize these energies. Thus, elucidating trends in metal–ligand properties is necessary for guiding catalyst development. The hallmark of efficient electrocatalysis—reversible reactivity—requires a flattened energy landscape.

The hallmark of efficient electrocatalysis—reversible reactivity—requires a flattened energy landscape.

Selectivity for CO<sub>2</sub> reduction in the presence of protons is a complex challenge due to multiple possible reaction pathways. To simplify, we have discussed the most commonly cited

mechanisms, detailing the thermodynamic parameters involved for each step and how they correlate with redox potential. We emphasize our generalized approach will not apply to all catalyst systems. Instead, we believe our analysis provides a useful framework for thoughtful and creative catalyst design and optimization. In the case of CO<sub>2</sub> reduction to CO, it is apparent that several key parameters are inversely related for single-site metals. However, these relationships can be broken using a secondary interaction, mirroring the approach used by a natural enzyme. Although it is not specifically discussed in our analysis, we also believe uncovering strategies for kinetic inhibition for undesirable reactions presents another fruitful area for targeted catalyst design.

In the case of CO<sub>2</sub> reduction to CO, it is apparent that several key parameters are inversely related for single-site metals. However, these relationships can be broken using a secondary interaction, mirroring the approach used by a natural enzyme.

## ASSOCIATED CONTENT

### Supporting Information

The Supporting Information is available free of charge on the ACS Publications website at DOI: 10.1021/acscentsci.9b00095.

Detailed tables with compound identity and references for data used in Figure 1 as well as a figure depicting hydricity values and the average two-electron reduction potential (PDF)

## AUTHOR INFORMATION

### Corresponding Author

\*E-mail: j.yang@uci.edu.

### ORCID

Jenny Y. Yang: 0000-0002-9680-8260

### Notes

The authors declare no competing financial interest.

## ACKNOWLEDGMENTS

J.M.B. and J.Y.Y. are supported by NSF Award 1554744. J.Y.Y. is also grateful for support as a Sloan Foundation Fellow and a CIFAR Azrieli Global Scholar.

## REFERENCES

- (1) Lewis, N. S.; Nocera, D. G. Powering the planet: Chemical challenges in solar energy utilization. *Proc. Natl. Acad. Sci. U. S. A.* **2006**, *103* (43), 15729–15735.
- (2) Gray, H. B. Powering the planet with solar fuel. *Nat. Chem.* **2009**, *1*, 7.
- (3) Kang, P.; Chen, Z.; Brookhart, M.; Meyer, T. J. Electrocatalytic reduction of carbon dioxide: let the molecules do the work. *Top. Catal.* **2015**, *58* (1), 30–45.
- (4) Seh, Z. W.; Kibsgaard, J.; Dickens, C. F.; Chorkendorff, I.; Nørskov, J. K.; Jaramillo, T. F. Combining theory and experiment in electrocatalysis: Insights into materials design. *Science* **2017**, *355* (6321), No. eaad4998.

- (5) Zhang, W.; Hu, Y.; Ma, L.; Zhu, G.; Wang, Y.; Xue, X.; Chen, R.; Yang, S.; Jin, Z. Progress and perspective of electrocatalytic CO<sub>2</sub> reduction for renewable carbonaceous fuels and chemicals. *Advanced Science* **2018**, *5* (1), 1700275.
- (6) Fisher, B. J.; Eisenberg, R. Electrocatalytic reduction of carbon dioxide by using macrocycles of nickel and cobalt. *J. Am. Chem. Soc.* **1980**, *102* (24), 7361–7363.
- (7) Tait, A. M.; Hoffman, M. Z.; Hayon, E. The reactivity of cobalt(I) complexes containing unsaturated macrocyclic ligands in aqueous solution. *J. Am. Chem. Soc.* **1976**, *98* (1), 86–93.
- (8) Gangi, D. A.; Durand, R. R. Binding of carbon dioxide to cobalt and nickel tetra-aza macrocycles. *J. Chem. Soc., Chem. Commun.* **1986**, *9*, 697–699.
- (9) Beley, M.; Collin, J. P.; Ruppert, R.; Sauvage, J. P. Electrocatalytic reduction of carbon dioxide by nickel cyclam<sup>2+</sup> in water: study of the factors affecting the efficiency and the selectivity of the process. *J. Am. Chem. Soc.* **1986**, *108* (24), 7461–7467.
- (10) Grant, J. L.; Goswami, K.; Spreer, L. O.; Otvos, J. W.; Calvin, M. Photochemical reduction of carbon dioxide to carbon monoxide in water using a nickel(II) tetra-azamacrocyclic complex as catalyst. *J. Chem. Soc., Dalton Trans.* **1987**, No. 9, 2105–2109.
- (11) Ishida, H.; Tanaka, H.; Tanaka, K.; Tanaka, T. Selective formation of HCOO<sup>-</sup> in the electrochemical CO<sub>2</sub> reduction catalysed by [Ru(bpy)<sub>2</sub>(CO)<sub>2</sub>]<sup>2+</sup> (bpy = 2,2'-bipyridine). *J. Chem. Soc., Chem. Commun.* **1987**, *2*, 131–132.
- (12) Collin, J. P.; Jouaiti, A.; Sauvage, J. P. Electrocatalytic properties of (tetraazacyclotetradecane)nickel(2+) and Ni<sub>2</sub>(biscyclam)<sup>4+</sup> with respect to carbon dioxide and water reduction. *Inorg. Chem.* **1988**, *27* (11), 1986–1990.
- (13) Creutz, C.; Schwarz, H. A.; Wishart, J. F.; Fujita, E.; Sutin, N. A dissociative pathway for equilibration of a hydrido CoL(H)<sup>2+</sup> complex with carbon dioxide and carbon monoxide. Ligand binding constants in the macrocyclic [14]-dienecobalt(I) system. *J. Am. Chem. Soc.* **1989**, *111* (3), 1153–1154.
- (14) Creutz, C.; Schwarz, H. A.; Wishart, J. F.; Fujita, E.; Sutin, N. Thermodynamics and kinetics of carbon dioxide binding to two stereoisomers of a cobalt(I) macrocycle in aqueous solution. *J. Am. Chem. Soc.* **1991**, *113* (9), 3361–3371.
- (15) Fujita, E.; Haff, J.; Sanzenbacher, R.; Elias, H. High electrocatalytic activity of RRSS-[NiIIHTIM](ClO<sub>4</sub>)<sub>2</sub> and [NiIIDMC](ClO<sub>4</sub>)<sub>2</sub> for carbon dioxide reduction (HTIM = 2,3,9,10-Tetramethyl-1,4,8,11-tetraazacyclotetradecane, DMC = C-meso-5,12-Dimethyl-1,4,8,11-tetraazacyclotetradecane). *Inorg. Chem.* **1994**, *33* (21), 4627–4628.
- (16) Kelly, C. A.; Blinn, E. L.; Camaioni, N.; D'Angelantonio, M.; Mulazzani, Q. G. Mechanism of CO<sub>2</sub> and H<sup>+</sup> reduction by Ni(cyclam)<sup>+</sup> in aqueous solution. A pulse and continuous radiolysis study. *Inorg. Chem.* **1999**, *38* (7), 1579–1584.
- (17) Smieja, J. M.; Benson, E. E.; Kumar, B.; Grice, K. A.; Seu, C. S.; Miller, A. J. M.; Mayer, J. M.; Kubiak, C. P. Kinetic and structural studies, origins of selectivity, and interfacial charge transfer in the artificial photosynthesis of CO. *Proc. Natl. Acad. Sci. U. S. A.* **2012**, *109* (39), 15646–15650.
- (18) Taheri, A.; Berben, L. A. Tailoring electrocatalysts for selective CO<sub>2</sub> or H<sup>+</sup> reduction: iron carbonyl clusters as a case study. *Inorg. Chem.* **2016**, *55* (2), 378–385.
- (19) Ramakrishnan, S.; Chidsey, C. E. D. Initiation of the electrochemical reduction of CO<sub>2</sub> by a singly reduced ruthenium(II) bipyridine complex. *Inorg. Chem.* **2017**, *56* (14), 8326–8333.
- (20) Nichols, A. W.; Chatterjee, S.; Sabat, M.; Machan, C. W. Electrocatalytic reduction of CO<sub>2</sub> to formate by an iron schiff base complex. *Inorg. Chem.* **2018**, *57* (4), 2111–2121.
- (21) Fogeron, T.; Todorova, T. K.; Porcher, J.-P.; Gomez-Mingot, M.; Chamoreau, L.-M.; Mellot-Draznieks, C.; Li, Y.; Fontecave, M. A bioinspired nickel(bis-dithiolene) complex as a homogeneous catalyst for carbon dioxide electroreduction. *ACS Catal.* **2018**, *8* (3), 2030–2038.
- (22) Dey, S.; Ahmed, M. E.; Dey, A. Activation of Co(I) state in a cobalt-dithiolato catalyst for selective and efficient CO<sub>2</sub> reduction to CO. *Inorg. Chem.* **2018**, *57* (10), 5939–5947.
- (23) Cometto, C.; Chen, L.; Anxolabéhère-Mallart, E.; Fave, C.; Lau, T.-C.; Robert, M. Molecular electrochemical catalysis of the CO<sub>2</sub>-to-CO conversion with a Co complex: A cyclic voltammetry mechanistic investigation. *Organometallics* **2018**, in press. DOI: 10.1021/acs.organo.8b00555
- (24) Yoo, C.; Kim, Y.-E.; Lee, Y. Selective transformation of CO<sub>2</sub> to CO at a single nickel center. *Acc. Chem. Res.* **2018**, *51* (5), 1144–1152.
- (25) Cometto, C.; Chen, L.; Lo, P.-K.; Guo, Z.; Lau, K.-C.; Anxolabéhère-Mallart, E.; Fave, C.; Lau, T.-C.; Robert, M. Highly selective molecular catalysts for the CO<sub>2</sub>-to-CO electrochemical conversion at very low overpotential. Contrasting Fe vs Co quaterpyridine complexes upon mechanistic studies. *ACS Catal.* **2018**, *8* (4), 3411–3417.
- (26) Kanega, R.; Onishi, N.; Wang, L.; Himeda, Y. Electroreduction of carbon dioxide to formate by homogeneous Ir catalysts in water. *ACS Catal.* **2018**, *8* (12), 11296–11301.
- (27) Nie, W.; McCrory, C. C. L. Electrocatalytic CO<sub>2</sub> reduction by a cobalt bis(pyridylmonoimine) complex: effect of acid concentration on catalyst activity and stability. *Chem. Commun.* **2018**, *54* (13), 1579–1582.
- (28) Göttle, A. J.; Koper, M. T. M. Determinant role of electrogenerated reactive nucleophilic species on selectivity during reduction of CO<sub>2</sub> catalyzed by metalloporphyrins. *J. Am. Chem. Soc.* **2018**, *140* (14), 4826–4834.
- (29) Liyanage, N. P.; Dulaney, H. A.; Huckaba, A. J.; Jurss, J. W.; Delcamp, J. H. Electrocatalytic reduction of CO<sub>2</sub> to CO with Re-pyridyl-NHCs: Proton source influence on rates and product selectivities. *Inorg. Chem.* **2016**, *55* (12), 6085–6094.
- (30) Francke, R.; Schille, B.; Roemelt, M. Homogeneously catalyzed electroreduction of carbon dioxide—Methods, mechanisms, and catalysts. *Chem. Rev.* **2018**, *118* (9), 4631–4701.
- (31) Takeda, H.; Cometto, C.; Ishitani, O.; Robert, M. Electrons, photons, protons and earth-abundant metal complexes for molecular catalysis of CO<sub>2</sub> reduction. *ACS Catal.* **2017**, *7* (1), 70–88.
- (32) Appel, A. M.; Bercaw, J. E.; Bocarsly, A. B.; Dobbek, H.; DuBois, D. L.; Dupuis, M.; Ferry, J. G.; Fujita, E.; Hille, R.; Kenis, P. J. A.; Kerfeld, C. A.; Morris, R. H.; Peden, C. H. F.; Portis, A. R.; Ragsdale, S. W.; Rauchfuss, T. B.; Reek, J. N. H.; Seefeldt, L. C.; Thauer, R. K.; Waldrop, G. L. Frontiers, opportunities, and challenges in biochemical and chemical catalysis of CO<sub>2</sub> fixation. *Chem. Rev.* **2013**, *113* (8), 6621–6658.
- (33) Berning, D. E.; Noll, B. C.; DuBois, D. L. Relative hydride, proton, and hydrogen atom transfer abilities of [HM(diphosphine)-<sub>2</sub>]PF<sub>6</sub> complexes (M = Pt, Ni). *J. Am. Chem. Soc.* **1999**, *121* (49), 11432–11447.
- (34) Raebiger, J. W.; DuBois, D. L. Thermodynamic studies of HRh(depx)<sub>2</sub> and [(H)2Rh(depx)<sub>2</sub>](CF<sub>3</sub>SO<sub>3</sub>): Relationships between five-coordinate monohydrides and six-coordinate dihydrides. *Organometallics* **2005**, *24* (1), 110–118.
- (35) Roberts, J. A. S.; Appel, A. M.; DuBois, D. L.; Bullock, R. M. Comprehensive thermochemistry of W–H bonding in the metal hydrides CpW(CO)<sub>2</sub>(IMes)H, [CpW(CO)<sub>2</sub>(IMes)H]<sup>•+</sup>, and [CpW(CO)<sub>2</sub>(IMes)(H)<sub>2</sub>]<sup>+</sup>. Influence of an N-heterocyclic carbene ligand on metal hydride bond energies. *J. Am. Chem. Soc.* **2011**, *133* (37), 14604–14613.
- (36) Chen, S.; Rousseau, R.; Raugé, S.; Dupuis, M.; DuBois, D. L.; Bullock, R. M. Comprehensive thermodynamics of nickel hydride Bis(diphosphine) complexes: A predictive model through computations. *Organometallics* **2011**, *30* (22), 6108–6118.
- (37) van der Eide, E. F.; Helm, M. L.; Walter, E. D.; Bullock, R. M. Structural and spectroscopic characterization of 17- and 18-electron piano-stool complexes of chromium. Thermochemical analyses of weak Cr–H bonds. *Inorg. Chem.* **2013**, *52* (3), 1591–1603.
- (38) Choi, J.; Pulling, M. E.; Smith, D. M.; Norton, J. R. Unusually weak metal–hydrogen bonds in HV(CO)<sub>4</sub>(P–P) and their



effectiveness as H• donors. *J. Am. Chem. Soc.* **2008**, *130* (13), 4250–4252.

(39) Tilset, M.; Parker, V. D. Solution homolytic bond dissociation energies of organotransition-metal hydrides. *J. Am. Chem. Soc.* **1989**, *111* (17), 6711–6717.

(40) Estes, D. P.; Vannucci, A. K.; Hall, A. R.; Lichtenberger, D. L.; Norton, J. R. Thermodynamics of the metal–hydrogen bonds in ( $\eta^5$ -C<sub>5</sub>H<sub>5</sub>)M(CO)<sub>2</sub>H (M = Fe, Ru, Os). *Organometallics* **2011**, *30* (12), 3444–3447.

(41) Matsubara, Y.; Fujita, E.; Doherty, M. D.; Muckerman, J. T.; Creutz, C. Thermodynamic and kinetic hydricity of ruthenium(II) hydride complexes. *J. Am. Chem. Soc.* **2012**, *134* (38), 15743–15757.

(42) Ciancanelli, R.; Noll, B. C.; DuBois, D. L.; DuBois, M. R. Comprehensive thermodynamic characterization of the metal–hydrogen bond in a series of cobalt-hydride complexes. *J. Am. Chem. Soc.* **2002**, *124* (12), 2984–2992.

(43) Fang, M.; Wiedner, E. S.; Dougherty, W. G.; Kassel, W. S.; Liu, T.; DuBois, D. L.; Bullock, R. M. Cobalt complexes containing pendant amines in the second coordination sphere as electrocatalysts for H<sub>2</sub> production. *Organometallics* **2014**, *33* (20), 5820–5833.

(44) Hu, Y.; Norton, J. R. Kinetics and Thermodynamics of H–/H•/H<sup>+</sup> transfer from a rhodium(III) hydride. *J. Am. Chem. Soc.* **2014**, *136* (16), 5938–5948.

(45) Barrett, S. M.; Pitman, C. L.; Walden, A. G.; Miller, A. J. M. Photoswitchable hydride transfer from iridium to 1-methylnicotinamide rationalized by thermochemical cycles. *J. Am. Chem. Soc.* **2014**, *136* (42), 14718–14721.

(46) Price, A. J.; Ciancanelli, R.; Noll, B. C.; Curtis, C. J.; DuBois, D. L.; DuBois, M. R. HRh(dppb)<sub>2</sub>, a powerful hydride donor. *Organometallics* **2002**, *21* (22), 4833–4839.

(47) Lilio, A. M.; Reineke, M. H.; Moore, C. E.; Rheingold, A. L.; Takase, M. K.; Kubiak, C. P. Incorporation of pendant bases into Rh(diphosphine)<sub>2</sub> complexes: Synthesis, thermodynamic studies, and catalytic CO<sub>2</sub> hydrogenation activity of [Rh(P<sub>2</sub>N<sub>2</sub>)<sub>2</sub>]<sup>+</sup> complexes. *J. Am. Chem. Soc.* **2015**, *137* (25), 8251–8260.

(48) Curtis, C. J.; Miedaner, A.; Ellis, W. W.; DuBois, D. L. Measurement of the hydride donor abilities of [HM(diphosphine)<sub>2</sub>]<sup>+</sup> complexes (M = Ni, Pt) by heterolytic activation of hydrogen. *J. Am. Chem. Soc.* **2002**, *124* (9), 1918–1925.

(49) Wiese, S.; Kilgore, U. J.; DuBois, D. L.; Bullock, R. M. [Ni(PMe<sub>2</sub>NPh<sub>2</sub>)<sub>2</sub>](BF<sub>4</sub>)<sub>2</sub> as an electrocatalyst for H<sub>2</sub> production. *ACS Catal.* **2012**, *2* (5), 720–727.

(50) Berning, D. E.; Miedaner, A.; Curtis, C. J.; Noll, B. C.; Rakowski DuBois, M. C.; DuBois, D. L. Free-energy relationships between the proton and hydride donor abilities of [HNi(diphosphine)<sub>2</sub>]<sup>+</sup> complexes and the half-wave potentials of their conjugate bases. *Organometallics* **2001**, *20* (9), 1832–1839.

(51) Curtis, C. J.; Miedaner, A.; Raebiger, J. W.; DuBois, D. L. Periodic trends in metal hydride donor thermodynamics: Measurement and comparison of the hydride donor abilities of the series HM(PNP)<sub>2</sub><sup>+</sup> (M = Ni, Pd, Pt; PNP = Et<sub>2</sub>PCH<sub>2</sub>N(Me)CH<sub>2</sub>PEt<sub>2</sub>). *Organometallics* **2004**, *23* (3), 511–516.

(52) Raebiger, J. W.; Miedaner, A.; Curtis, C. J.; Miller, S. M.; Anderson, O. P.; DuBois, D. L. Using ligand bite angles to control the hydricity of palladium diphosphine complexes. *J. Am. Chem. Soc.* **2004**, *126* (17), 5502–5514.

(53) Miedaner, A.; Raebiger, J. W.; Curtis, C. J.; Miller, S. M.; DuBois, D. L. Thermodynamic studies of [HPt(EtXantphos)<sub>2</sub>]<sup>+</sup> and [(H)<sub>2</sub>Pt(EtXantphos)<sub>2</sub>]<sup>2+</sup>. *Organometallics* **2004**, *23* (11), 2670–2679.

(54) Morris, R. H. Estimating the acidity of transition metal hydride and dihydrogen complexes by adding ligand acidity constants. *J. Am. Chem. Soc.* **2014**, *136* (5), 1948–1959.

(55) Sung, M. M. H.; Jdanova, S.; Morris, R. H. Ligand acidity constants as calculated by density functional theory for PF<sub>3</sub> and N-Heterocyclic carbene ligands in hydride complexes of Iron(II). *J. Organomet. Chem.* **2019**, *880*, 15–21.

(56) Morris, R. H. Brønsted–Lowry acid strength of metal hydride and dihydrogen complexes. *Chem. Rev.* **2016**, *116* (15), 8588–8654.

(57) Wang, D.; Angelici, R. J. Metal–hydrogen bond dissociation enthalpies in series of complexes of eight different transition metals. *J. Am. Chem. Soc.* **1996**, *118* (5), 935–942.

(58) Fu, X.; Wayland, B. B. Thermodynamics of rhodium hydride reactions with CO, aldehydes, and olefins in water: Organo-rhodium porphyrin bond dissociation free energies. *J. Am. Chem. Soc.* **2005**, *127* (47), 16460–16467.

(59) Rakowski Dubois, M.; Dubois, D. L. Development of molecular electrocatalysts for CO<sub>2</sub> reduction and H<sub>2</sub> production/oxidation. *Acc. Chem. Res.* **2009**, *42* (12), 1974–1982.

(60) DuBois, D. L.; Berning, D. E. Hydricity of transition-metal hydrides and its role in CO<sub>2</sub> reduction. *Appl. Organomet. Chem.* **2000**, *14* (12), 860–862.

(61) Wiedner, E. S.; Chambers, M. B.; Pitman, C. L.; Bullock, R. M.; Miller, A. J. M.; Appel, A. M. Thermodynamic hydricity of transition metal hydrides. *Chem. Rev.* **2016**, *116* (15), 8655–8692.

(62) Waldie, K. M.; Ostericher, A. L.; Reineke, M. H.; Sasayama, A. F.; Kubiak, C. P. Hydricity of transition-metal hydrides: Thermodynamic considerations for CO<sub>2</sub> reduction. *ACS Catal.* **2018**, *8* (2), 1313–1324.

(63) Bullock, R. M.; Appel, A. M.; Helm, M. L. Production of hydrogen by electrocatalysis: making the H–H bond by combining protons and hydrides. *Chem. Commun.* **2014**, *50* (24), 3125–3143.

(64) Ceballos, B. M.; Yang, J. Y. Directing the reactivity of metal hydrides for selective CO<sub>2</sub> reduction. *Proc. Natl. Acad. Sci. U. S. A.* **2018**, *115* (50), 12686–12691.

(65) Tsay, C.; Ceballos, B. M.; Yang, J. Y., pH-dependent reactivity of a water-soluble nickel complex: Hydrogen evolution vs selective electrochemical hydride generation. *Organometallics* **2018**, in press. DOI: 10.1021/acs.organomet.8b00558

(66) Tsay, C.; Yang, J. Y. Electrocatalytic hydrogen evolution under acidic aqueous conditions and mechanistic studies of a highly stable molecular catalyst. *J. Am. Chem. Soc.* **2016**, *138* (43), 14174–14177.

(67) DuBois, D. L. Development of molecular electrocatalysts for energy storage. *Inorg. Chem.* **2014**, *53* (8), 3935–3960.

(68) Smith, S. E.; Yang, J. Y.; DuBois, D. L.; Bullock, R. M. Reversible electrocatalytic production and oxidation of hydrogen at low overpotentials by a functional hydrogenase mimic. *Angew. Chem., Int. Ed.* **2012**, *51* (13), 3152–3155.

(69) Priyadarshani, N.; Dutta, A.; Ginovska, B.; Buchko, G. W.; O'Hagan, M.; Rauegi, S.; Shaw, W. J. Achieving reversible H<sub>2</sub>/H<sup>+</sup> interconversion at room temperature with enzyme-inspired molecular complexes: A mechanistic study. *ACS Catal.* **2016**, *6* (9), 6037–6049.

(70) Dutta, A.; Appel, A. M.; Shaw, W. J. Designing electrochemically reversible H<sub>2</sub> oxidation and production catalysts. *Nature Reviews Chemistry* **2018**, *2* (9), 244–252.

(71) Taheri, A.; Thompson, E. J.; Fettinger, J. C.; Berben, L. A. An iron electrocatalyst for selective reduction of CO<sub>2</sub> to formate in water: Including thermochemical insights. *ACS Catal.* **2015**, *5* (12), 7140–7151.

(72) Ceballos, B. M.; Tsay, C.; Yang, J. Y. CO<sub>2</sub> reduction or HCO<sub>2</sub>-oxidation? Solvent-dependent thermochemistry of a nickel hydride complex. *Chem. Commun.* **2017**, *53* (53), 7405–7408.

(73) Creutz, C.; Chou, M. H. Rapid transfer of hydride ion from a ruthenium complex to C1 species in water. *J. Am. Chem. Soc.* **2007**, *129* (33), 10108–10109.

(74) Muckerman, J. T.; Achord, P.; Creutz, C.; Polyansky, D. E.; Fujita, E. Calculation of thermodynamic hydricities and the design of hydride donors for CO<sub>2</sub> reduction. *Proc. Natl. Acad. Sci. U. S. A.* **2012**, *109* (39), 15657–15662.

(75) Brereton, K. R.; Pitman, C. L.; Cundari, T. R.; Miller, A. J. M. Solvent-dependent thermochemistry of an iridium/ruthenium H<sub>2</sub> evolution catalyst. *Inorg. Chem.* **2016**, *55* (22), 12042–12051.

(76) Tsay, C.; Livesay, B. N.; Ruelas, S.; Yang, J. Y. Solvation effects on transition metal hydricity. *J. Am. Chem. Soc.* **2015**, *137* (44), 14114–14121.

(77) Burgess, S. A.; Appel, A. M.; Linehan, J. C.; Wiedner, E. S. Changing the mechanism for CO<sub>2</sub> hydrogenation using solvent-

dependent thermodynamics. *Angew. Chem., Int. Ed.* **2017**, *56* (47), 15002–15005.

(78) Loewen, N. D.; Neelakantan, T. V.; Berben, L. A. Renewable formate from C–H bond formation with CO<sub>2</sub>: Using iron carbonyl clusters as electrocatalysts. *Acc. Chem. Res.* **2017**, *50* (9), 2362–2370.

(79) Kang, P.; Zhang, S.; Meyer, T. J.; Brookhart, M. Rapid selective electrocatalytic reduction of carbon dioxide to formate by an iridium pincer catalyst immobilized on carbon nanotube electrodes. *Angew. Chem., Int. Ed.* **2014**, *53* (33), 8709–8713.

(80) Kang, P.; Cheng, C.; Chen, Z.; Schauer, C. K.; Meyer, T. J.; Brookhart, M. Selective electrocatalytic reduction of CO<sub>2</sub> to formate by water-stable iridium dihydride pincer complexes. *J. Am. Chem. Soc.* **2012**, *134* (12), 5500–5503.

(81) Roy, S.; Sharma, B.; Pécaut, J.; Simon, P.; Fontecave, M.; Tran, P. D.; Derat, E.; Artero, V. Molecular cobalt complexes with pendant amines for selective electrocatalytic reduction of carbon dioxide to formic acid. *J. Am. Chem. Soc.* **2017**, *139* (10), 3685–3696.

(82) Ogata, T.; Yanagida, S.; Brunschwig, B. S.; Fujita, E. Mechanistic and kinetic studies of cobalt macrocycles in a photochemical CO<sub>2</sub> reduction system: Evidence of Co–CO<sub>2</sub> adducts as intermediates. *J. Am. Chem. Soc.* **1995**, *117* (25), 6708–6716.

(83) Schmidt, M. H.; Miskelly, G. M.; Lewis, N. S. Effects of redox potential, steric configuration, solvent, and alkali metal cations on the binding of carbon dioxide to cobalt(I) and nickel(I) macrocycles. *J. Am. Chem. Soc.* **1990**, *112* (9), 3420–3426.

(84) Fujita, E.; Creutz, C.; Sutin, N.; Szalda, D. J. Carbon dioxide activation by cobalt(I) macrocycles: factors affecting carbon dioxide and carbon monoxide binding. *J. Am. Chem. Soc.* **1991**, *113* (1), 343–353.

(85) Froehlich, J. D.; Kubiak, C. P. The homogeneous reduction of CO<sub>2</sub> by [Ni(cyclam)]<sup>+</sup>: Increased catalytic rates with the addition of a CO scavenger. *J. Am. Chem. Soc.* **2015**, *137* (10), 3565–3573.

(86) Isse, A. A.; Gennaro, A.; Vianello, E.; Floriani, C. Electrochemical reduction of carbon dioxide catalyzed by [CoI(salophen)Li]. *J. Mol. Catal.* **1991**, *70* (2), 197–208.

(87) Schneider, J.; Jia, H.; Muckerman, J. T.; Fujita, E. Thermodynamics and kinetics of CO<sub>2</sub>, CO, and H<sup>+</sup> binding to the metal centre of CO<sub>2</sub> reduction catalysts. *Chem. Soc. Rev.* **2012**, *41* (6), 2036–2051.

(88) Balazs, G. B.; Anson, F. C. Effects of CO on the electrocatalytic activity of Ni(cyclam)<sub>2</sub><sup>+</sup> toward the reduction of CO<sub>2</sub>. *J. Electroanal. Chem.* **1993**, *361* (1–2), 149–157.

(89) Shaffer, D. W.; Johnson, S. I.; Rheingold, A. L.; Ziller, J. W.; Goddard, W. A.; Nielsen, R. J.; Yang, J. Y. Reactivity of a series of isostructural cobalt pincer complexes with CO<sub>2</sub>, CO, and H<sup>+</sup>. *Inorg. Chem.* **2014**, *53* (24), 13031–13041.

(90) Hansen, H. A.; Varley, J. B.; Peterson, A. A.; Nørskov, J. K. Understanding trends in the electrocatalytic activity of metals and enzymes for CO<sub>2</sub> reduction to CO. *J. Phys. Chem. Lett.* **2013**, *4* (3), 388–392.

(91) Leitner, W. The coordination chemistry of carbon dioxide and its relevance for catalysis: a critical survey. *Coord. Chem. Rev.* **1996**, *153* (0), 257–284.

(92) Gibson, D. H. The organometallic chemistry of carbon dioxide. *Chem. Rev.* **1996**, *96* (6), 2063–2096.

(93) Aresta, M.; Nobile, C. F.; Albano, V. G.; Forni, E.; Manassero, M. New nickel-carbon dioxide complex: synthesis, properties, and crystallographic characterization of (carbon dioxide)-bis-(tricyclohexylphosphine)nickel. *J. Chem. Soc., Chem. Commun.* **1975**, *15*, 636–637.

(94) Dohring, A.; Jolly, P. W.; Kruger, C.; Romão, M. J. The Ni(0)-CO<sub>2</sub> system: Structure and reactions of [Ni(PCy<sub>3</sub>)<sub>2</sub>(n<sub>2</sub>-CO<sub>2</sub>)]. *Z. Naturforsch., B: J. Chem. Sci.* **1985**, *40B*, 484–488.

(95) Mason, M. G.; Ibers, J. A. Reactivity of some transition metal systems toward liquid carbon dioxide. *J. Am. Chem. Soc.* **1982**, *104* (19), 5153–5157.

(96) Aresta, M.; Nobile, C. F. (Carbon dioxide)bis-(trialkylphosphine)nickel complexes. *J. Chem. Soc., Dalton Trans.* **1977**, No. 7, 708–711.

(97) Hammouche, M.; Lexa, D.; Momenteau, M.; Saveant, J. M. Chemical catalysis of electrochemical reactions. Homogeneous catalysis of the electrochemical reduction of carbon dioxide by iron(“0”) porphyrins. Role of the addition of magnesium cations. *J. Am. Chem. Soc.* **1991**, *113* (22), 8455–8466.

(98) Maher, J. M.; Cooper, N. J. Reduction of carbon dioxide to carbon monoxide by transition-metal dianions. *J. Am. Chem. Soc.* **1980**, *102* (25), 7604–7606.

(99) Lee, G. R.; Maher, J. M.; Cooper, N. J. Reductive disproportionation of carbon dioxide by dianionic carbonylmetalates of the transition metals. *J. Am. Chem. Soc.* **1987**, *109* (10), 2956–2962.

(100) Chatt, J.; Kubota, M.; Leigh, G. J.; March, F. C.; Mason, R.; Yarrow, D. J. A possible carbon dioxide complex of molybdenum and its rearrangement product di-[small micro]-carbonato-bis-{carbonyltris(dimethylphenylphosphine)molybdenum}: X-ray crystal structure. *J. Chem. Soc., Chem. Commun.* **1974**, *24*, 1033–1034.

(101) Karsch, H. H. Funktionelle trimethylphosphinderivate, III. Ambivalentes Verhalten von tetrakis(trimethylphosphin)eisen: Reaktion mit CO<sub>2</sub>. *Chem. Ber.* **1977**, *110* (6), 2213–2221.

(102) Evans, G. O.; Walter, W. F.; Mills, D. R.; Streit, C. A. Reactions of carbon dioxide with metal carbonyl anions. *J. Organomet. Chem.* **1978**, *144* (2), C34–C38.

(103) Machan, C. W.; Chabolla, S. A.; Yin, J.; Gilson, M. K.; Tezcan, F. A.; Kubiak, C. P. Supramolecular assembly promotes the electrocatalytic reduction of carbon dioxide by Re(I) bipyridine catalysts at a lower overpotential. *J. Am. Chem. Soc.* **2014**, *136* (41), 14598–14607.

(104) Sullivan, B. P.; Bolinger, C. M.; Conrad, D.; Vining, W. J.; Meyer, T. J. One- and two-electron pathways in the electrocatalytic reduction of CO<sub>2</sub> by fac-Re(bpy)(CO)<sub>3</sub>Cl (bpy = 2,2′-bipyridine). *J. Chem. Soc., Chem. Commun.* **1985**, *20*, 1414–1416.

(105) Bolinger, C. M.; Story, N.; Sullivan, B. P.; Meyer, T. J. Electrocatalytic reduction of carbon dioxide by 2,2′-bipyridine complexes of rhodium and iridium. *Inorg. Chem.* **1988**, *27* (25), 4582–4587.

(106) Sampson, M. D.; Froehlich, J. D.; Smieja, J. M.; Benson, E. E.; Sharp, I. D.; Kubiak, C. P. Direct observation of the reduction of carbon dioxide by rhenium bipyridine catalysts. *Energy Environ. Sci.* **2013**, *6* (12), 3748–3755.

(107) Yang, W.; Sinha Roy, S.; Pitts, W. C.; Nelson, R. L.; Fronczek, F. R.; Jurss, J. W. Electrocatalytic CO<sub>2</sub> reduction with Cis and Trans conformers of a rigid dinuclear rhenium complex: Comparing the monometallic and cooperative bimetallic pathways. *Inorg. Chem.* **2018**, *57* (15), 9564–9575.

(108) Parkin, A.; Seravalli, J.; Vincent, K. A.; Ragsdale, S. W.; Armstrong, F. A. Rapid and efficient electrocatalytic CO<sub>2</sub>/CO interconversions by Carboxydotherrmus Hydrogenoformans CO dehydrogenase I on an electrode. *J. Am. Chem. Soc.* **2007**, *129* (34), 10328–10329.

(109) Jeoung, J.-H.; Dobbek, H. Carbon dioxide activation at the Ni<sub>2</sub>Fe-cluster of anaerobic carbon monoxide dehydrogenase. *Science* **2007**, *318* (5855), 1461–1464.

(110) Can, M.; Armstrong, F. A.; Ragsdale, S. W. Structure, function, and mechanism of the nickel metalloenzymes, CO dehydrogenase, and Acetyl-CoA synthase. *Chem. Rev.* **2014**, *114* (8), 4149–4174.

(111) Majumdar, A. Bioinorganic modeling chemistry of carbon monoxide dehydrogenases: description of model complexes, current status and possible future scopes. *Dalton Trans* **2014**, *43*, 12135–12145.

(112) Raebiger, J. W.; Turner, J. W.; Noll, B. C.; Curtis, C. J.; Miedaner, A.; Cox, B.; DuBois, D. L. Electrochemical reduction of CO<sub>2</sub> to CO catalyzed by a bimetallic palladium complex. *Organometallics* **2006**, *25* (14), 3345–3351.

(113) Steffey, B. D.; Curtis, C. J.; DuBois, D. L. Electrochemical reduction of CO<sub>2</sub> catalyzed by a dinuclear palladium complex containing a bridging hexaphosphine ligand: Evidence for cooperativity. *Organometallics* **1995**, *14* (10), 4937–4943.



- (114) Dubois, D. L. Development of transition metal phosphine complexes as electrocatalysts for CO<sub>2</sub> and CO reduction. *Comments Inorg. Chem.* **1997**, *19* (5), 307–325.
- (115) DuBois, D. L.; Miedaner, A.; Haltiwanger, R. C. Electrochemical reduction of carbon dioxide catalyzed by [Pd(tri-phosphine)-(solvent)](BF<sub>4</sub>)<sub>2</sub> complexes: synthetic and mechanistic studies. *J. Am. Chem. Soc.* **1991**, *113* (23), 8753–8764.
- (116) Krogman, J. P.; Foxman, B. M.; Thomas, C. M. Activation of CO<sub>2</sub> by a heterobimetallic Zr/Co complex. *J. Am. Chem. Soc.* **2011**, *133* (37), 14582–14585.
- (117) Fachinetti, G.; Floriani, C.; Zanazzi, P. F. Bifunctional activation of carbon dioxide. Synthesis and structure of a reversible carbon dioxide carrier. *J. Am. Chem. Soc.* **1978**, *100* (23), 7405–7407.
- (118) Gambarotta, S.; Arena, F.; Floriani, C.; Zanazzi, P. F. Carbon dioxide fixation: bifunctional complexes containing acidic and basic sites working as reversible carriers. *J. Am. Chem. Soc.* **1982**, *104* (19), 5082–5092.
- (119) Cooper, O.; Camp, C.; Pécaut, J.; Kefalidis, C. E.; Maron, L.; Gambarelli, S.; Mazzanti, M. Multimetallic cooperativity in uranium-mediated CO<sub>2</sub> activation. *J. Am. Chem. Soc.* **2014**, *136* (18), 6716–6723.
- (120) Lim, C.-H.; Holder, A. M.; Hynes, J. T.; Musgrave, C. B. Roles of the Lewis acid and base in the chemical reduction of CO<sub>2</sub> catalyzed by frustrated Lewis pairs. *Inorg. Chem.* **2013**, *52* (17), 10062–10066.
- (121) Hattori, T.; Suzuki, Y.; Miyano, S. Lewis acid-mediated carboxylation of aryl- and allylsilanes with carbon dioxide. *Chem. Lett.* **2003**, *32* (5), 454–455.
- (122) Menard, G.; Stephan, D. W. CO<sub>2</sub> reduction via aluminum complexes of ammonia boranes. *Dalton Trans* **2013**, *42* (15), 5447–5453.
- (123) Fachinetti, G.; Floriani, C.; Zanazzi, P. F.; Zanzari, A. R. Bifunctional model complexes active in carbon dioxide fixation: synthesis and x-ray structure of bimetallic cobalt(I)-alkali cation-Schiff base complexes. *Inorg. Chem.* **1979**, *18* (12), 3469–3475.
- (124) Bhugun, I.; Lexa, D.; Savéant, J.-M. Catalysis of the electrochemical reduction of carbon dioxide by iron(0) porphyrins. Synergistic effect of Lewis acid cations. *J. Phys. Chem.* **1996**, *100* (51), 19981–19985.
- (125) Fujita, E.; Szalda, D. J.; Creutz, C.; Sutin, N. Carbon dioxide activation: thermodynamics of carbon dioxide binding and the involvement of two cobalt centers in the reduction of carbon dioxide by a cobalt(I) macrocycle. *J. Am. Chem. Soc.* **1988**, *110* (14), 4870–4871.
- (126) Pinkes, J. R.; Steffey, B. D.; Vites, J. C.; Cutler, A. R. Carbon dioxide insertion into the iron-zirconium and ruthenium-zirconium bonds of the heterobimetallic complexes Cp(CO)<sub>2</sub>MZr(Cl)Cp<sub>2</sub>: direct production of the  $\mu$ - $\eta^1$ (C)- $\eta^2$ (O,O')-CO<sub>2</sub> compounds Cp(CO)<sub>2</sub>MCO<sub>2</sub>Zr(Cl)Cp<sub>2</sub>. *Organometallics* **1994**, *13* (1), 21–23.
- (127) Fujita, E.; Creutz, C.; Sutin, N.; Brunschwig, B. S. Carbon dioxide activation by cobalt macrocycles: evidence of hydrogen bonding between bound CO<sub>2</sub> and the macrocycle in solution. *Inorg. Chem.* **1993**, *32* (12), 2657–2662.
- (128) Costentin, C.; Drouet, S.; Robert, M.; Savéant, J.-M. A local proton source enhances CO<sub>2</sub> electroreduction to CO by a molecular Fe catalyst. *Science* **2012**, *338* (6103), 90–94.
- (129) Chapovetsky, A.; Welborn, M.; Luna, J. M.; Haiges, R.; Miller, T. F.; Marinescu, S. C. Pendant hydrogen-bond donors in cobalt catalysts independently enhance CO<sub>2</sub> reduction. *ACS Cent. Sci.* **2018**, *4* (3), 397–404.
- (130) Azcarate, I.; Costentin, C.; Robert, M.; Savéant, J.-M. Through-space charge interaction substituent effects in molecular catalysis leading to the design of the most efficient catalyst of CO<sub>2</sub>-to-CO electrochemical conversion. *J. Am. Chem. Soc.* **2016**, *138* (51), 16639–16644.
- (131) Sung, S.; Kumar, D.; Gil-Sepulcre, M.; Nippe, M. Electrocatalytic CO<sub>2</sub> reduction by imidazolium-functionalized molecular catalysts. *J. Am. Chem. Soc.* **2017**, *139* (40), 13993–13996.
- (132) Froehlich, J. D.; Kubiak, C. P. Homogeneous CO<sub>2</sub> reduction by Ni(cyclam) at a glassy carbon electrode. *Inorg. Chem.* **2012**, *51* (7), 3932–3934.
- (133) Chapovetsky, A.; Do, T. H.; Haiges, R.; Takase, M. K.; Marinescu, S. C. Proton-assisted reduction of CO<sub>2</sub> by cobalt aminopyridine macrocycles. *J. Am. Chem. Soc.* **2016**, *138* (18), 5765–5768.
- (134) DeLuca, E. E.; Xu, Z.; Lam, J.; Wolf, M. O., Improved electrocatalytic CO<sub>2</sub> reduction with palladium bis(NHC) pincer complexes bearing cationic side chains. *Organometallics*. **2018** DOI: 10.1021/acs.organomet.8b00649.